

PRECIPITATION IN THE ZIRCONIUM - 1.5wt% TIN BASE ALLOY

O.M.Nešić, V.M.Stefanović and Ž.Lj.Spasić
Boris Kidrič Institute of Nuclear Sciences, Beograd

Introduction

Due to their good mechanical, nuclear and corrosion resistance properties, zirconium - tin base alloys are extensively used in the reactor technology. Since the power reactor safety must be guaranteed over a number of years, it is necessary to have reliable information on the microstructure characteristics (precipitates, defects, etc.) and fatigue properties of alloys. Since the formed hydride exhibits a predominant role on the crack nucleation, extensive studies of hydrogen precipitation in zirconium alloys have been made(1,2). Bailey(1) reviewed and studied morphology and crystallographic parameters of hydride precipitates, while the effects of hydride precipitates on the fatigue crack nucleation were examined by Wohnile et al.,(2). In the present work the electron transmission microscopy has been used to observe the precipitates in the fully annealed alloy, as a part of the test program of the effects of fatigue and irradiation on tensile properties.

Zirconium - Tin System

The solubility of tin in α -Zr decreases from 9% at 980°C, to 1.5% at 600°C. On further cooling the solubility of tin decreases to very small values. Pure low-tin zirconium alloys have an intermetallic phase Zr_4Sn with 24.55wt%Sn, which is formed during peritectoid reaction at 1325°C(3). However, Ostberg(4) suggests that beta to alpha transformation in the zirconium 1.5wt%Sn alloy with impurities (zircaloy) is of the eutectoid rather than the peritectoid type. The relatively large contents of impurities present in these alloys made it nearly impossible to detect the initial appearance of the Zr_4Sn phase which precipitates as a very fine dispersion of particles in the zirconium matrix. According to McPherson and Hansen(3) Zr_4Sn phase is f.c.tetragonal lattice with parameters $a = 7.645\text{\AA}$, $c = 12.461\text{\AA}$, $c/a = 1.63$; according to Miller(5) these parameters are : $a = 6.90\text{\AA}$, $c = 11.10\text{\AA}$, $c/a = 1.63$.

Material

All the specimens were taken from cold-rolled plates delivered by "Cefilax"

Chemical Analysis, wt.-%				
Sn	1.48	Fe	0.13	} <0.28
O	1200 ppm	Cr	0.10	
N	37 ppm	Ni	0.05	

Annealing treatments were performed at 1250⁰C for 2hs in the vacuum of 10₆ Torr. After heat treatment the sample of the alloy was subjected to X-ray analysis. The resulting pattern indicates the increase of the parameter c(=5.1477A) to 0=5.152A as compared to pure zirconium(6), a = 3.231A, c/a = 1.59.

Indexing electron diffraction pattern, we obtained for the same parameters : a = 3.24A, c = 5.15A, c/a = 1.588.

Preparation of Thin Foils

To obtain thin foils specimens were mechanically ground to a thickness of 0.2 mm, and then electropolished with 1:4 perchloric/acetic acid solution, at less than 10⁰C, at a potential of 15V. Thin foils were examined under polarized light and in a JEM-7 electron microscope, operating at 100 kV.

Observation

Metallographic examination under polarized light shows that the cold-rolled texture of α -grains was eliminated by the applied heat treatment. The equi-axed β -grain size of a fully annealed alloy varied from 1 to 3mm in diameter. The "basketweave" structure, Fig.1, typical for many zirconium alloys was produced by random precipitation of α -plates on a number of equivalent lattice habit planes in one β -grain. The plates expand by thickening with rejection of the alloying elements. Small particles, such as carbides(7,8) may serve as nucleation sites for α -plates and influence "basketweave" structure appearance in the alloys. The alloy contains a dispersion of coarse second phase particles on α -plates boundaries.

Transmission electron microscope observation indicated that the homogeneous and heterogeneous precipitations of the second phase are present in the alloy. Homogeneous precipitation resulted in the appearance of fine precipitates in the zirconium matrix, while the heterogeneous precipitation produced many

coarse particles in the α -plates interfaces. Some coarse precipitates electron diffraction patterns show the streaks that proves the presence of defects such as thin twins or stacking faults, Fig. 2. Their diffraction patterns were indexed as tetragonal lattice with parameters $a = 7.247\text{\AA}$, $c = 14.51\text{\AA}$, $c/a \approx 2$. Comparing these values to those found in the literature (3), we could suppose that in spite of the difference in parameters, observed precipitates are the Zr_4Sn phase modified due to high impurity content in the alloy.

Figure 3(a,b) illustrates the homogeneous precipitation of fine particles in the α -zirconium matrix. Bright and dark-field images and electron diffraction patterns show that thin rod-shaped precipitates, Fig. 3a, depending on their size might be coherent or partly-coherent to the matrix. Under the favorable diffraction conditions a semi-circular "halo"-type contrast appears on one or both sides of precipitates, due to the coherency strains induced in the matrix surrounding the precipitates, Fig. 3b. A similar effect has been observed on hydride precipitates (1) and GP-2 zones (9). Due to close relationship, the precipitate spots are usually in some way associated to the matrix spots, indicating the matrix periodicity modulation, Fig. 4. On several electron diffraction patterns, the rod-shaped particles spots could be indexed as tetragonal lattice with following parameters: $a = 7.35\text{\AA}$, $c = 12.03\text{\AA}$, $c/a = 1.635$. These values are very close to those published by McPherson and Hansen (3) for Zr_4Sn .

It is interesting to note that morphology and crystallographic parameters for thin rod-shaped particles with their long axes parallel to $(11\bar{2}0)_\alpha$ and $(10\bar{1}0)_\alpha$ directions, and habit planes $\{10\bar{1}0\}_\alpha$, $\{10\bar{1}1\}_\alpha$ and $\{11\bar{2}0\}_\alpha$ determined by trace analysis, are identical to those for hydride precipitates in hydrided zirconium alloy (1). However, hydride precipitation in the matrix was not positively identified, except for small surface foil precipitates usually attached to twins and dislocation lines, and appeared as dislocation loops noncoherent to the matrix; which gave no distinct diffraction spots and might be the hydrogen atoms agglomerates, probably formed during foil preparation (1).

Summary

1. In fully beta-annealed Zr-1.5wt%Sn, at room temperature, two types of precipitates exist:
 - a. coarse particles distributed at alpha-plates boundaries, and
 - b. fine homogeneously distributed rod-like precipitates with their long axes parallel to $(11\bar{2}0)_\alpha$ and $(10\bar{1}0)_\alpha$ directions.
 2. Crystallographic parameters for rod-like precipitates, directions and habit planes $\{10\bar{1}0\}_\alpha$, $\{10\bar{1}1\}_\alpha$ and $(11\bar{2}0)_\alpha$ are the same as for zirconium hydride precipitates.
 3. High impurity content suppresses pure Zr_4Sn phase precipitation.
- Summarizing observations we could expect that, due to their fine precipitates homogeneously distributed throughout the matrix and many coarse precipitates in alpha-plates boundaries, fully annealed Zr-1.5wt%Sn alloys are susceptible to brittle fracture.

Literature

1. Y.E.Bailey: Acta Met., 11(1963)267
2. r.J.H.Wohnle, O.H.Ryder, R.Davies: J.Inst.Met., 96(1968)59
3. J.D.McPherson, M.Hansen: Trans. ASM, 45(1953)915
4. O.J.Ostberg: Jernkontorets Ann., 195(1963)71
5. G.H.Miller: "Zirconium", Butterworths Sci. Pub. Co., 1957, London, p.369
6. W.B.Pearson: "Handbook of lattice spacing and structure of metals", Pergamon Press, London, 1963
7. G.Okvist, K.Källström: J.Nucl.Mat., 35(1970)316
8. A.R.Halt: J.Nucl.Mat., 35(1970)322
9. R.B.Nicholson, R.B.Nutting: Phil.Mag., 11(1963)267



FIG.1.

"Basketweave" structure in β -annealed Zr-1.48wt% Sn alloy. Polishing: perchloric/acetic acid solution. Polarized light.



FIG.2.

Electron micrograph. Coarse α -plate boundary precipitates and corresponding electron diffraction pattern.

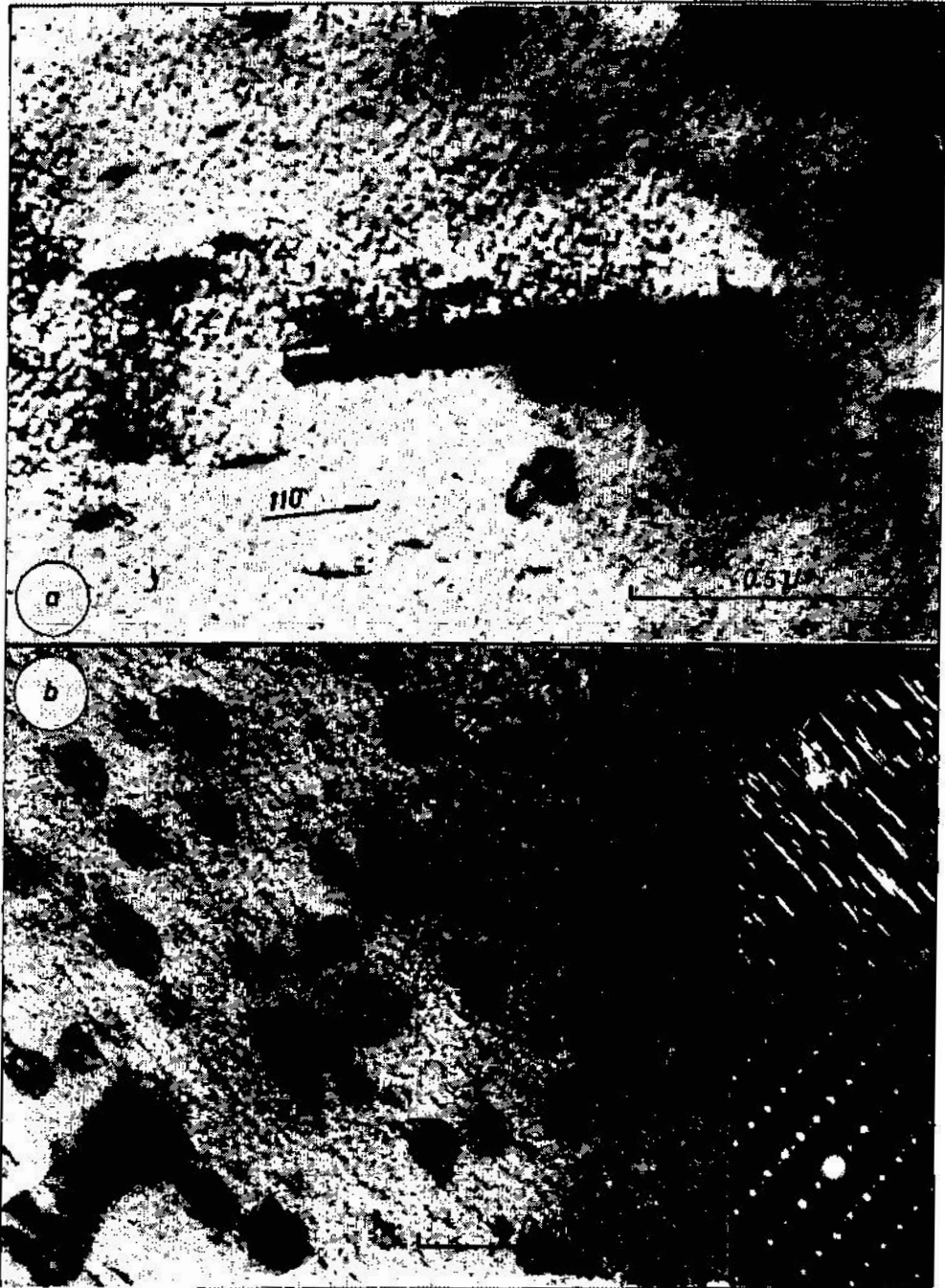


FIG. 3.

Electron micrograph of homogeneously distributed precipitates
 (a). Rod-like precipitate along $(11\bar{2}0)_\alpha$ direction.
 (b). Matrix strain field contrast. Bright- and dark-field images
 and the corresponding electron diffraction pattern.

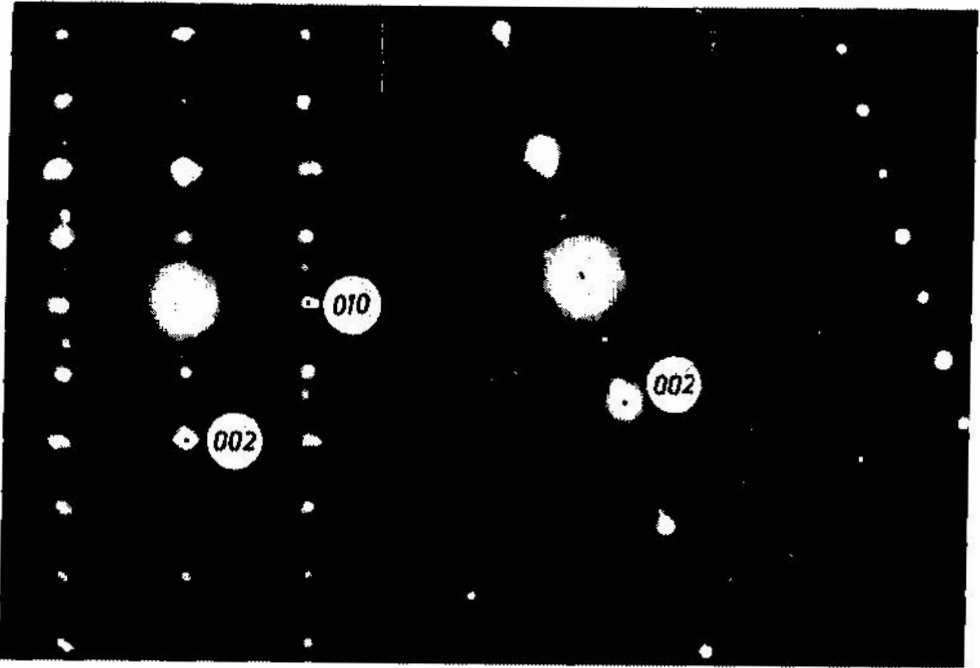


FIG. 4.

Electron diffraction patterns from fine precipitates.

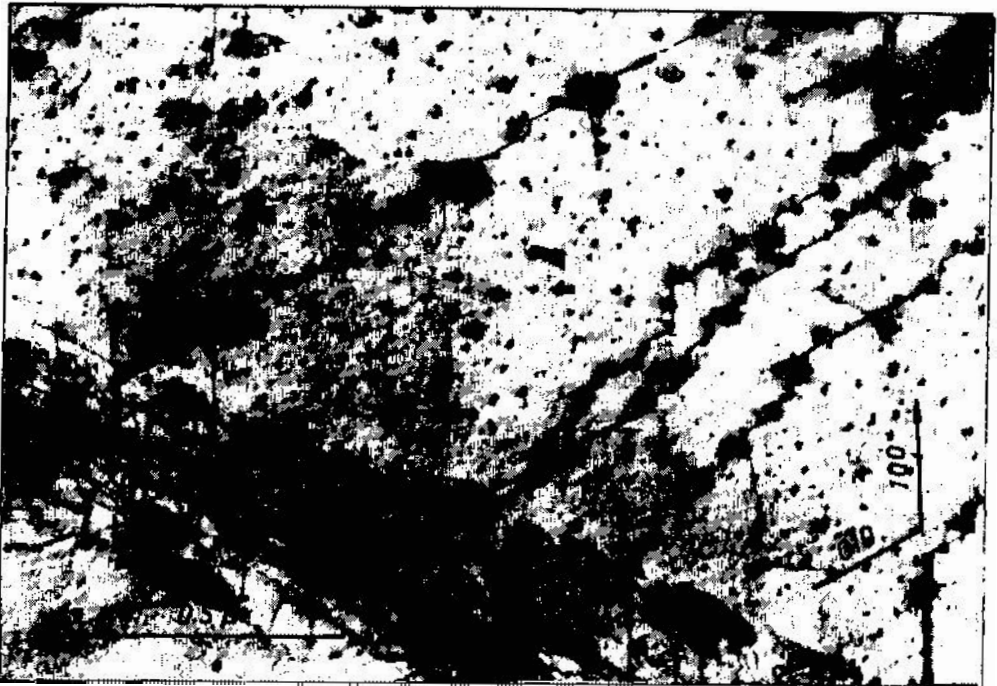


FIG. 5.

Foil surface precipitates attached to dislocation lines.

DISCUSSION

- H. Warlimont : What is the nature of the finely dispersed features visible in the matrix phase on your electron micrographs ?
- V. Stefanović : According to our diffraction pattern the side band appeared round the (001) direction, spots indicating the spinodal decomposition throughout the specimen.
- G. Lorimer : Have you tried to form a dark field image with the "side-bands" observed in the diffraction pattern ?
- V. Stefanović : Yes, we did, and the structure did show up in the dark field.